
Article:
Yao, D, Wu, C, Yang, H et al. (5 more authors) (2017) Co-production of hydrogen and carbon nanotubes from catalytic pyrolysis of waste plastics on Ni-Fe bimetallic catalyst. Energy Conversion and Management, 148. pp. 692-700. ISSN 0196-8904

https://doi.org/10.1016/j.enconman.2017.06.012

Co-production of hydrogen and carbon nanotubes from catalytic pyrolysis of waste plastics on Ni-Fe bimetallic catalyst

Dingding Yao[a], Chunfei Wu[b,**], Haiping Yang[a,*], Yeshui Zhang[c], Mohamad A. Nahil[c], Yingquan Chen[a], Paul T. Williams[c], Hanping Chen[a]

[a] *State Key Laboratory of Coal Combustion, School of Energy and Power Engineering, Huazhong University of Science and Technology, 430074 Wuhan, China*

[b] *School of Engineering and Computer Science, University of Hull, Hull HU6 7RX UK*

[c] *School of Chemical and Process Engineering, University of Leeds, Leeds, LS2 9JT, UK*

ABSTRACT

To explore the mechanism of the influence of Ni-Fe bimetallic catalyst for the producing high-value carbon nanotubes (CNTs) with clean hydrogen from waste plastic pyrolysis, the pyrolysis-catalysis of plastics were performed using a two stage fixed bed reaction system with Ni and Fe loading at variant molar ratios. The catalysts and produced carbon were analyzed with various characterization method, including temperature-programed reduction/oxidation, X-ray diffraction, scanning electron microscopy or/and Raman spectroscopy. Both the H_2 concentration and H_2 yield reached maximum values of 73.93 vol.% and 84.72 mg g^{-1} plastic, respectively, as the ratio of Ni：Fe at 1:3. The amount and quality of CNTs were greatly influenced by the catalyst composition, and Ni and Fe display different roles to the overall reactivity of Ni-Fe catalyst for the pyrolysis-catalysis of waste plastics. Catalyst with more Fe

* Corresponding authors. E-mail address: yhping2002@163.com (Haiping Yang); C.Wu@hull.ac.uk (Chunfei Wu)

loading produced more hydrogen and deposited carbon, due to higher cracking ability and the relatively lower interaction between active sites and support. The presence of Ni in Ni-Fe bimetallic catalyst enhanced the thermal stability and graphitization degree of produced carbons. The thermal quality of filamentous carbons might be associated with carbon defects.

Keywords： waste plastics, hydrogen, carbon nanotubes, Ni-Fe bimetallic catalyst

1. Introduction

The global demand for plastic increases annually as the rapid economic development and higher standard of living. However, the increased use of plastic materials produces substantial quantities of plastic and brings serious environmental problems. In China, approximately 18 million tons of plastic wastes were generated in 2015 [1]. It was reported that 25 million tonnes of wastes plastics are generated annually in Europe, and more than 30% of post-consumer waste plastics end up in landfill or incineration [2, 3].

Energy recovery like pyrolysis of plastics for chemical products is a promising way to exploit the full potential of waste plastics. The thermal and catalytic pyrolysis of plastics have been extensively studied in different reactors and under various operational parameters, with the product distributions being dependent on these conditions [4, 5]. Williams et al. [6] reported that pyrolysis waxes and oil enriched in aliphatic composition could be produced from low density polyethylene using a fluidised bed reactor. Ratnasari et al. [7] obtained a gasoline range hydrocarbons yield

of 83.15 wt.% from waste plastics in a staged catalysis system with MCM-41 and ZSM-5. In addition, waste plastics could also be gasified [8] or co-gasified with biomass [9] for hydrogen production at high catalyst temperatures. There has been increasing interest in the pyrolysis-catalysis of waste plastics for high-value-added products. Recently, carbon nanomaterials like CNTs have been obtained with catalysis-pyrolysis of waste plastics [10, 11]. In that process, the valuable product CNTs was produced instead of unwanted coke, which may lead to serious catalyst deactivation. Furthermore, low-cost CNTs from waste plastics have been used as reinforced material and resulted good performance of tensile and flexural strength, presenting its great potential in industry application [12, 13].

CNTs, since it was firstly reported by Iijima in the early 1990s [14], has been attracting considerable attentions because of the unique electrochemical and mechanical properties [15]. It is known that CH_4, C_2H_2 that from petrol industry, are normally used as the carbon precursors for carbon nanotubes production using chemical vapor deposition (CVD) method, which has been the dominant mode for large production around the world [16-18]. As those small gases for CNTs production can also be obtained from pyrolysis of waste plastics, it is an attractive way to apply the pyrolysis-catalysis process to waste plastics for carbon nanotubes without overdue consumption of non-renewable resources. Pyrolysis-catalysis process of waste plastics for producing CNTs has similar principle as traditional CVD method using CH_4, whereas, the main difference is that pyrolysis of plastic produces complicated carbon sources. Ni based catalysts are reported to have good reactivity for C-C and C-H bond

cleavage, thus they are effective for polymers cracking and reforming reactions [19, 20]. Zhang et al. [21] found that Ni/Al_2O_3 showed higher activity to multi-walled CNTs production along with higher H_2 yield compared to Co/Al_2O_3 and Cu/Al_2O_3 for the catalytic reforming of waste tires. Yang et al. [22] synthesized CNTs with 20~30 diameter in a pilot-scale system using $H\text{-}Ni/Al_2O_3$ catalyst, demonstrating the feasibility of Ni based catalyst for treating plastics continuously to generate high value CNTs. Bulk carbon deposition of highly uniform carbon nanotubes as well as 55% of hydrogen yield were observed from methane catalytic decomposition with Ni/La2O3 catalyst by Pudukudy et al. [23]. Besides, Fe based catalyst is also an attractive catalyst with cheap and environmental friendly traits for the production of carbon nanotubes. Acomb et al. [24] investigated the influence of different metal catalysts for catalytic pyrolysis of LDPE, and found that Fe/Al_2O_3 gave the highest H_2 conversion (26.8 %) and carbon yield (26 wt.%), compared with Ni, Co and Cu based catalysts. The moderate metal-support interaction and irons large carbon solubility contributed to its good performance.

For many catalysts studies, bimetallic catalysts by integrating different materials are always suggested when considering both catalytic reactivity and energy consumption. Some bimetallic catalysts like Ni-Mg, Ni-Mn [12] and Fe-Ru [25] have been studied for the filamentous carbon production from pyrolysis-catalysis of polymers. Ni was suggested to be responsible for the formation of carbon nanotubes while Mn acted as a favorable promoter during carbon growth. The interaction between Cu and Fe was found to enhance the nucleation of nanotubes over Fe as well

as minimize the bulk accumulation of carbon substrates [26]. The advantages of those bimetallic or trimetallic catalysts always come from good stability, smaller metal particle size and appropriate interaction or synergy between metals [27].

As for the Ni-Fe bimetallic catalysts, it has shown favorable performance for some studies. Ni-Fe based on bio-char has been performed into biomass gasification to increase tar conversion in an effective and economical way [28]. H_2 yield and carbon conversion rate were increased when using Fe-Ni oxides were used for pine sawdust gasification, resulting from the synergistic effect between Fe_2O_3 and NiO [29]. Enhanced methane dehydrogenation and longer life-times activity of catalyst were found by Shen et al. [30] when using Ni-Fe/Mg(Al)O for CNTs production from methane. However, there are limited reports about using Ni-Fe bimetallic catalysts for the coproduction of CNTs and H_2 from waste plastics. Furthermore, the role of Ni or Fe on CNT and H_2 production are still unclear. Therefore, the catalytic pyrolysis of waste plastic was investigated the bimetallic Ni-Fe catalyst for the simultaneous production of H_2 and carbon nanotubes using a two-stage fixed bed reactor. In order to understand the different catalytic reactivity, the prepared catalysts and solid products were characterized by spectroscopic, temperature programmed and electronic microscope analysis. Gas releasing behavior, H_2 yield, morphology and quality of solid carbon at different Ni to Fe molar ratio were examined.

2. Experimental material and methods

2.1 Experimental materials

The waste plastics used in this research are some disposable drink cups, lunch boxes, and plastic wraps (Mingjin Plastic Ltd, China), which are widely used for food packing in daily life. They were crushed and mixed using a liquid nitrogen grinder with particle size between 0.1 and 0.5 mm. The composition was 40 wt.% sample bottles (mainly HDPE), 35 wt.% plastic bags (mainly LDPE), 20 wt.% preservative boxes (mainly PP) and 5 wt.% lunch boxes (mainly PS). The ultimate analysis of the material was 84.51 wt.% C, 13.85 wt.% H, 1.51 wt.% O and 0.13 wt.% S. Ash content of the mixed plastics was less than 1 wt.%.

Bimetallic Ni-Fe catalysts with different Ni to Fe molar ratio were prepared using impregnation method. Metal nitrates and gamma Al_2O_3 (obtained from Sigma Aldrich, UK) were used as the materials. The initial metal loading was 10 wt.%. As an example, $Ni(NO_3)_3{\cdot}6H_2O$ and $Fe(NO_3)_3{\cdot}9H_2O$ were firstly dissolved in ethanol with Ni to Fe molar ratio of 1 to 3, then 10g gamma Al_2O_3 was added. Then the precursors were stirred for 4 h using magnetic stirrer at 50 °C, and dried at 100 °C overnight, followed by calcination at 800 °C for 3 hours holding time under air atmosphere with a heating rate of 10 C min^{-1}. The other catalysts were prepared following the same procedure, but with different Ni to Fe ratio. It need to be pointed out that no reduction prior to the catalytic pyrolysis as the gases produced during pyrolysis-catalytic process such as H_2 and CH_4 might reduce the metal oxides in situ [31]. The five catalysts prepared here were denoted as NiFe13, NiFe12, NiFe11, NiFe21 and NiFe31 separately (corresponding to the molar ratio of Ni:Fe of 1:3, 1:2, 1:1, 2:1 and 3:1).

2.2 Experimental setup and procedure

The pyrolysis-catalytic process of waste plastics was carried out in a two-stage fixed bed reactor (Fig. 1). The reaction system consists essentially of a quartz tube reactor (I.D. 40mm) with two temperature ranges (upper: pyrolysis zone, 310 mm height; under: catalysis zone, 310 mm height), a gas supplying system, gaseous product condensing system with ice and water mixture, a gas cleaning system followed by gas online and offline measurement system.

Before each experiment, 0.5g catalyst was supported by ~0.2g stainless steel wire mesh on the top of a perforated plate, which was placed in the middle of second stage, where the temperature was heated to 800 °C. A quartz basket with 1g waste plastic was hold in the top of first reactor. High purity of Argon (99.99%) was supplied as inert gas at 110ml min^{-1}. After the catalyst temperature reached to selected temperature and kept stable, the basket containing plastic sample was introduced into the middle of first stage, and the pyrolysis temperature was programmed to increase from room temperature to 500 °C with a heating rate of 10 °C min^{-1} and held at 500°C for 15 min. After pyrolysis-catalytic process, condensable vapors were collected by a two-stage ice-water condenser. A small branch of the non-condensable gases was introduced into mass spectrometer (MS) (Ominstar TM－GSD320, Pfeiffer Vaccum, Germany) to monitor gas evolution online with a data acquisition frequency of 1 s^{-1}. The signals identified as the atomic mass units of 2, 16, 26, 28, 30, 44 corresponded to the main produced gas H_2, CH_4, C_2H_2, $CO+C_2H_4$, C_2H_6 and CO_2 respectively, according to the molecular weights of gases. The main stream was sampled with a 20

L gasbag, and gas composition was determined using a dual-channel gas chromatograph (GC) (Micro-GC 3000A, Agilent Technology, USA) equipped with thermal conductivity detectors. H_2, CO and CH_4 were detected by channel A (molecular sieve 5A) and CO_2, C_2H_2, C_2H_4, C_2H_6 were measured by channel B (polystyrene chromatographic column). Each experiment was repeated twice to ensure the reliability of the results.

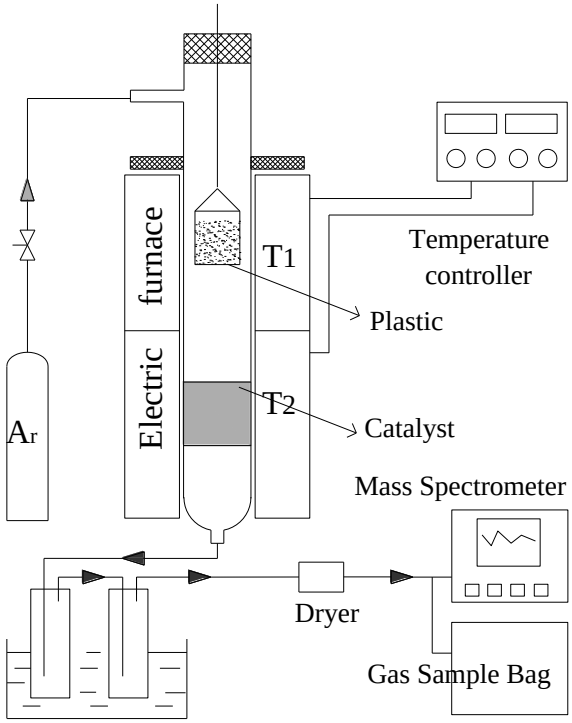

Fig. 1. Schematic diagram of the pyrolysis-catalysis process of waste plastics.

2.3 Catalyst characterization

Crystal structure and species identification of the fresh catalysts were determined by a X-ray diffraction (XRD) analyzer (X'Pert PRO, PANalytical B.V., Netherlands), with a scanning step of 0.026° in the 2θ range from 5° to 85°. Peaks were identified using High Score Plus software package. Temperature programmed reduction (TPR)

was also performed to characterize the fresh catalyst in a Shimadzu thermo gravimetric analyzer (TGA). Approximately 30 mg of catalyst sample was preheated to 150 °C at a heating rate of 20 °C min-1 and held for 30 min in reduction atmosphere (5 % H_2 / 95 % N_2), and then heated to 900 °C at 10 °C min^{-1}. The BET surface area of the five Ni/Fe catalysts were calculated from N_2 adsorption and desorption isotherms on an automatic adsorption equipment (ASAP2020, Micromeritics, USA) operating at 77K.

The morphologies of CNTs were obtained using a scanning electron microscopy (SEM) operating at 20 kV (JSM-5610LV, JEOL, Japan), and transmission electron microscope (TEM) observation was also carried out on a FEI Tecnai TF20. The thermal stability of carbon deposited on the catalysts was determined with temperature-programmed oxidation (TPO) in a TGA (PerkinElmer Instruments, USA). A total of 10 mg of the reacted catalyst was heated from room temperature to 800 °C in air (100 ml min^{-1}) with a heating rate of 10 °C min^{-1} and a holding time of 10 min at 800 °C. Raman spectroscopy of deposited carbon was carried out to determine the graphitic quality. And the spectrograms were obtained using a LabRAM HR800 (Horiba JobinYvon, Japan) Raman spectrometer at a wavelength of 532 nm with Raman shift from 200 to 3500 cm^{-1}.

2.4 Analysis methods

Concentrations of the gases collected in the sample bag were obtained from gas chromatography, and then the mass of each gas could be calculated based on the

concentrations and flow rate of carrier gas. Carbon deposition (solid) production was determined as the mass difference between fresh and reacted catalyst. The liquid yield of each experiment was obtained from the weight difference of the condenser before and after the experimental test. The total gas, liquid and carbon deposition yields were calculated by each product in relation to the total weight of waste plastics. Mass balance was then obtained based on the sum of gas, liquid and solid yield to check the reliability of each experiment. The mass balance in the presence of catalyst showed good results, ranging from 95.7 to 101.4 wt.%, and a standard deviation of 0.22 vol. % of gas content was obtained for the repeated experiments. In order to better present the hydrogen conversion from plastic, H_2 yield was defined as the mass of H_2 in the product gas divided by the theoretical H content in the feedstock according to the ultimate analysis.

3. Results and discussion

3.1 Characterization of fresh catalyst

BET surface area of the fresh catalysts was 112.71, 109.72, 111.68, 106.90, 104.07 $m^2 g^{-1}$ for the catalyst NiFe13, NiFe12, NiFe11, NiFe21, NiFe31 respectively, and the BJH average pore diameter was much similar in the range of 50 to 58 Å. It seems these five catalysts were prepared with similar structure properties. The crystalline structure of the fresh prepared Ni-Fe catalysts was shown in Fig. 2. There are notable differences of crystal composition between catalysts with different Ni to Fe ratio. Iron was observed with different oxidation state. The diffraction peak of

Fe_2O_3 was obviously detected with NiFe13. Both of Ni-Al and Fe-Al spinel were observed, indicating the interaction between active metals and support, it is a key factor for CNT production [24]. For NiFe12, the intensity of Fe_2O_3 was weak while more Fe_3O_4 with a relatively lower valence state of Fe was found. And at higher ratio of Ni to Fe, the peak of Fe_2O_3 can hardly been detected. It seems that the exiting of Ni lead to part reduction of ferric iron, which might influence the reduction or cracking ability of catalyst.

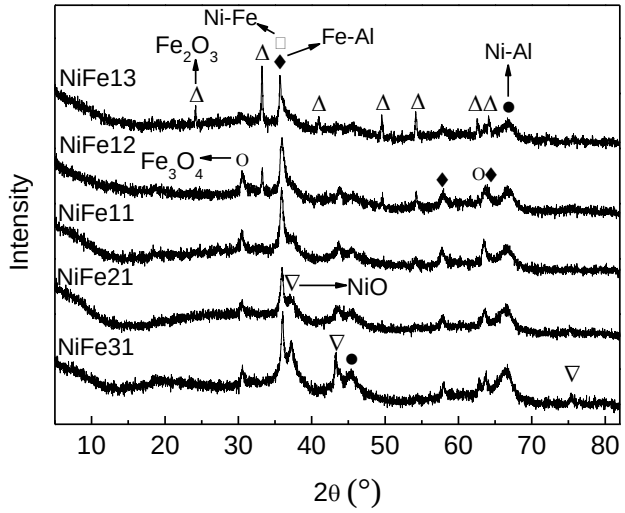

Fig. 2. X-ray diffraction profiles of the fresh Ni-Fe catalysts.

The reduction of Ni-Fe bimetallic catalysts is complex and presents in a number of asymmetric stages (Fig.3). TPR results of NiFe13 show a peak around 400 °C in addition to a broader peak from 500 to 750 °C and a peak higher than 750 °C. It suggests that more than two metal species contributes to the reduction of NiFe13. According to Al-Dossary et al. [32], the reduction of Fe_2O_3 undergoes two or even three steps with the following sequence and occur in specified temperatures:

229 $$Fe_2O_3 \rightarrow Fe_3O_4 \rightarrow [FeO] \rightarrow Fe^0 \quad (1)$$

230 The first step was reported corresponding to the reduction of hematite into
231 magnetite, it mainly happens at around 400 °C. Further, it is reduced into [FeO]
232 (wustite, unstable) and metallic Fe occur at high temperatures and they always coexist,
233 which means it may produce some asymmetric and overlapped peaks [24, 32]. And
234 reduction kinetics change from chemical to diffusion controlling mechanism because
235 of high metal loading always lead to a higher reduction peak [33]. In order to classify
236 the reduction process clearly, four stages of reduction are indicated in Fig. 3.
237 Therefore, in this work, H_2 consumption peak observed at stage I belongs to the
238 reduction of Fe_2O_3 into Fe_3O_4, while the H_2 consumption at stage III was caused by
239 the subsequent reduction of Fe_3O_4 into FeO or Fe. For the NiFe12 and NiFe11, the
240 tiny peak at lower temperature suggests that the catalyst is not easy to be reduced,
241 indicating a strong interaction between metal and support. This is consistent with the
242 XRD results (Fig. 2) that Ni and Fe display a co-spinel state with support, and less
243 Fe_2O_3 or NiO was found. A peak at stage II can be seen for Ni-Fe bimetallic catalysts
244 at higher Ni to Fe ratio, and it attributes to the reduction of free NiO which interacts
245 weakly to y-Al_2O_3 [34]. In addition, the peak intensity turns higher for NiFe31, and
246 results are consistent with the XRD results that more NiO sites are detected at high Ni
247 loading. NiFe31 also presents an obvious peak from 550 to 600 °C, which is related to
248 the reduction of NiO with high interaction with support according to [35]. All the five
249 catalysts show a reduction peak above 750 °C (stage IV), which is associated to a
250 spinel-metal phase where Ni or Fe has migrated into the support Al_2O_3 and is hardly

to be reduced [36]. In addition, as the hydrogen consumption of this metal-spinel increased with the rising Ni to Fe ratio and it can be seen a larger proportion of Ni in case of Ni-Al spinel than Fe in the Fe-Al spinel from TPR results, the overall interaction between metal oxides and Al_2O_3 was enhanced with the rising Ni to Fe ratio.

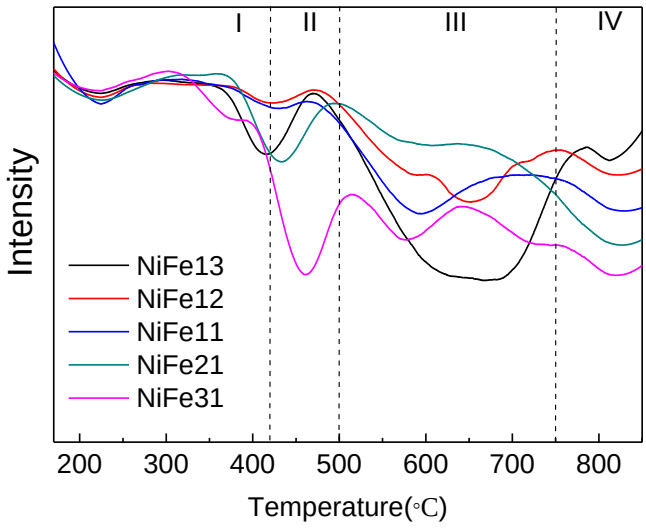

Fig. 3. Temperature programmed reduction profiles of the fresh Ni-Fe catalysts.

3.2 Gas releasing property of catalytic pyrolysis of waste plastics

For each experiment, less than 0.001g of pyrolysis char (~0.1 wt.%) was left for each experiment (the balance has 1 mg readability), indicating that the plastics were almost converted into vapours completely. Information about product evolution and distribution can be obtained by means of mass spectrometer analysis. Ion-current changes versus time during pyrolysis-catalytic process of plastics with/without catalysts are shown in Fig. 4, and real-time temperature for each trial was also plotted. As the oxygen content of plastics was very limited and oxygenic groups exist in side

chain of polymer, it is suggested that oxygen-contained compounds like CO and CO_2 are easily released at the beginning of the reaction. In that sense, for the signal of 28 a.m.u, which is the superposition of C_2H_4 and CO, the first peak was due to the evolution of CO and the second was for the C_2H_4. It can be seen that gas from only thermal cracking of plastic wastes (the no catalyst trial in Fig.4 (a)) mainly consist of CH_4, C_2H_4. While CH_4 and C_2H_4 have been reported as good carbon sources for the catalytic reaction for the production of CNTs [37], it is effective to use the Ni-Fe catalyst for the following carbon formation reactions. When Ni-Fe catalysts were applied, more H_2 was produced, with the maximum value achieved in the range of 430 to 450 °C. However, as the H_2 maximum peak without catalyst was around 420 °C, it seems that the gas release when using catalysts was delayed slightly. It may due to the fact that more complexed reactions happened like catalyst redox and carbon deposition. The ion intensity of C_2H_4 was considerably weak during the whole catalysis process and it can be identified from the overlapped peak. It can be seen NiFe12 and NiFe13 have higher H_2 selectivity than other catalysts as the plotted line of H_2 was much higher than that of other gases. Gas emissions are similar at higher ratio of Ni to Fe. The gas was released in the following order: CO_x (x=1, 2), H_2, CxHy (including CH_4, C_2H_4, C_2H_2 and other hydrocarbons).

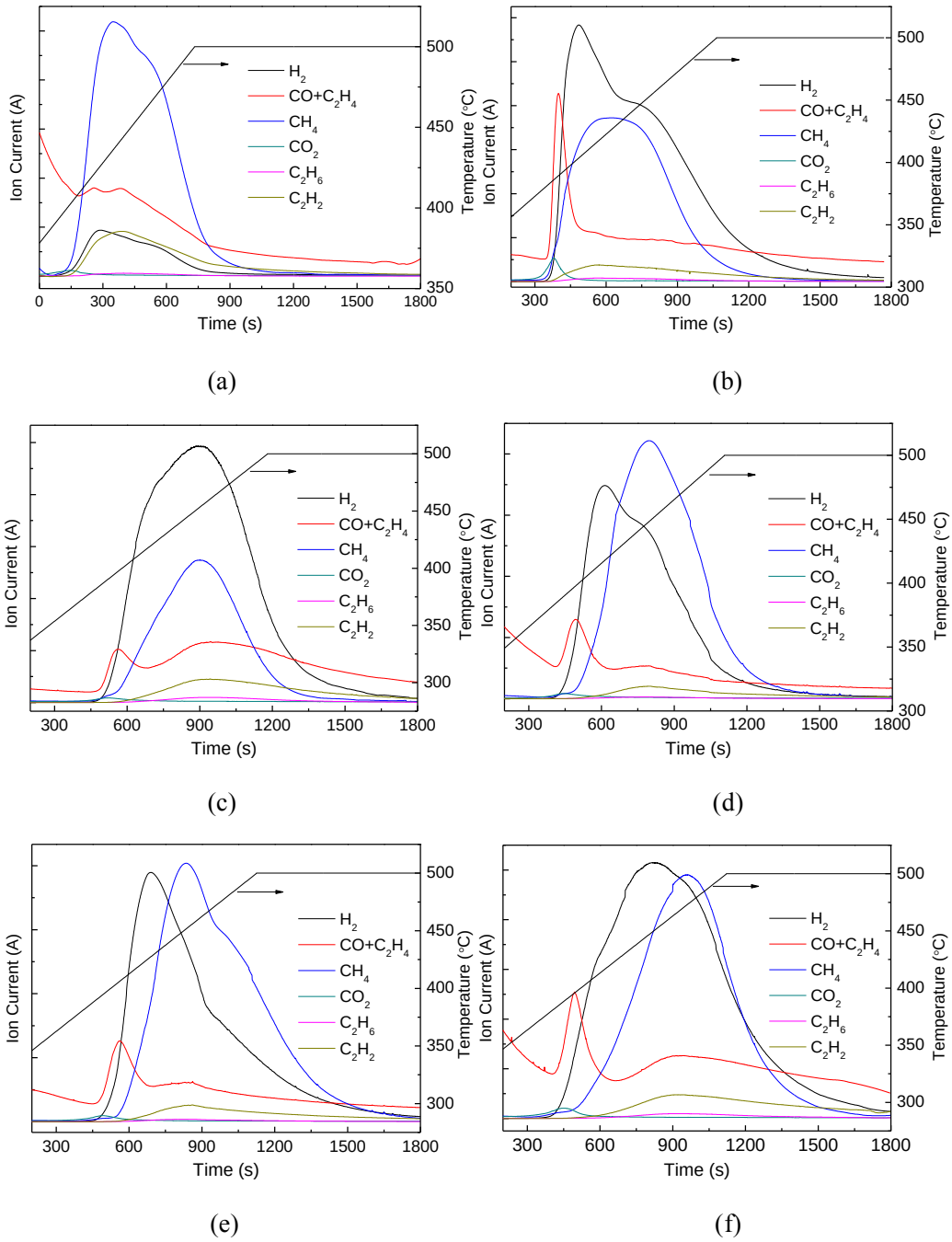

Fig. 4. Gas releasing behaviours during the pyrolysis-catalysis process of waste plastics. (a) no catalyst, (b) NiFe13, (c) NiFe12, (d) NiFe11, (e) NiFe21, (f) NiFe31.

In order to compare these five catalysts in terms of different products quantities, the gas yield, gas composition, solid yield as well as mass balance are summarized in Table 1. Pyrolysis of waste plastics resulted in 50.51 wt.% gas yield, 2.2 wt.% carbon

299 deposits and 11.42 % hydrogen yield without catalyst (sand was used in place of
300 catalyst). The mass balance was 80.51 wt.% in the absence of catalyst. The low mass
301 balance may due to the inadequate decomposition of pyrolysis vapours that condensed
302 on the walls of reactor or converted to hydrocarbon gases which were hard to be
303 collected. H_2 yield was significantly increased using Ni-Fe bimetallic catalysts, and
304 reached maximum value of 61.17 % (84.72 mg g^{-1} plastic) in the presence of NiFe13
305 catalyst. The lowest H_2 yield of 48.92 % was obtained with NiFe21 among all the
306 catalytic experiments. Regarding the total gas yield, catalysts with higher Ni to Fe
307 ratio showed relatively higher activity for total gas production than NiFe13 and
308 NiFe12, while the trend was opposite for the yield of carbon deposition. The carbon
309 deposition using NiFe13 was 50.9 wt.%，which was higher than that of NiFe11,
310 NiFe21 or NiFe31 (about 45 wt.%). It appears that NiFe13 and NiFe12, which contain
311 more Fe species, are more favorable for carbon deposits, than those catalysts with Ni
312 to Fe ratio higher than 1. It may due to the fact that the interaction between
313 metal-support of NiFe13 is moderately weak (from TPR results), and result in a high
314 yield of carbons [38]. This result agrees well with Acomb et al. [24], who found
315 Fe/Al_2O_3 generated a higher yield of carbon deposits than Ni/Al_2O_3 during
316 pyrolysis-catalytic process of low density polyethylene.

317 Table 1 also shows the volumetric content of gases. The controlled trial without
318 catalyst generated the highest amount of CH_4 and C_2H_4, with a content of 49.36
319 vol. % and 19.81 vol.%, respectively. And the content of CH_4 was twice of H_2, which
320 was consistent with the releasing trend observed in Fig. 4. The introduced five Ni-Fe

catalysts reduced hydrocarbon gases and accordingly increased H_2 content as a result of the catalytic cracking reactions (Reaction (2)). As more C was converted into solid state instead of gaseous product with the catalytic cracking reactions, hence the lower gas yield was observed with catalysts adding. The highest (73.93 vol.%) content of H_2 was observed over NiFe13 catalyst, followed by NiFe12 and NiFe31, with the H_2 content of 73.59 vol.% and 69.98 vol.%, respectively. It suggested the highest cracking ability of NiFe13, which was attribute to the presence of many reducible metal oxides observed from XRD (Fig. 2) and TPR (Fig. 3) results. NiFe11 and NiFe21 produced the relatively lower hydrogen content (around 64 vol.%) and higher CH_4 content (around 27 vol.%) among five Ni-Fe catalysts, which was also found in Fig. 4.

$$C_xH_y \rightarrow x\ C + (y/2)\ H_2 \tag{2}$$

Table 1

Mass balance and gas production with different Ni-Fe catalysts.

	No catalyst[1]	NiFe13	NiFe12	NiFe11	NiFe21	NiFe31
H_2 yield (%)	11.42	61.17	56.15	49.85	48.92	52.30
Gas yield (wt. %)	50.51	39.48	38.01	43.24	43.87	39.64
Carbon deposits (wt. %)	2.2	50.9	49.9	45.8	45.1	45.8
Liquid yield (wt.%)	27.8	8.8	13.5	7.1	9.9	10.3
Mass balance (%)	80.51	99.18	101.41	96.14	98.87	95.74
Gas composition (vol. %)						
H_2	24.74	73.93	73.59	64.81	63.84	69.98
CO	2.98	3.90	3.74	4.19	3.76	4.37
CH_4	49.36	16.77	15.12	26.40	27.16	19.15
CO_2	0.67	0.62	0.64	0.77	0.65	0.76
C_2H_4	19.81	3.43	4.88	3.12	3.60	4.15
C_2H_6	2.24	1.30	1.97	0.63	0.92	1.56
C_2H_2	0.20	0.04	0.05	0.08	0.07	0.04

[1]: T_1=500 °C, T_2=800 °C, 0.5g silica sand.

3.3 Carbon nanotubes production

The oxidation properties of carbon nanomaterial obtained from the surface of used catalyst samples were studied by temperature-programmed oxidation (TPO) as shown in Fig. 5. According to the loss weight ratio of catalysts after oxidation, the metal residues increased from 40 wt.% to 52 wt.% when Ni to Fe ratio increased from 1:3 to 3:1, suggesting a lower amount of metal-assisted carbon growth with more Ni loading. It is consistent with the previous carbon yield results (Table 2) that NiFe13 catalysts produced the higher carbon deposits. The derivative TPO plots show that most of the carbons were oxidized after 550 °C. Acomb at al [39] defined two types of carbon with oxidation temperature in his work, where a lower temperature of TPO peak from 350 to 450 °C was related to amorphous carbons and a higher temperature between 500 and 700 °C was associated to the filamentous carbons. Yang et al. [22] assigned the weight loose at 500 to the amorphous carbon, and the oxidation at 600 to 700 to the multi-walled CNTs. As such, most of carbons formed in this study were filamentous carbons. The carbon deposited on catalyst became less reactive when Ni to Fe molar ratio increased, as the oxidation peak from DTG plots moved to higher temperature with Ni content increased. It indicates that Ni composition in the catalyst enhanced the thermal stability and graphitization of formed carbons. Sivakular et al. [40] synthesized Ni and Fe catalysts on active carbon for multi-walled carbon nanotubes production from methane, and reported that CNTs formed on Ni exhibited higher thermal stability than Fe.

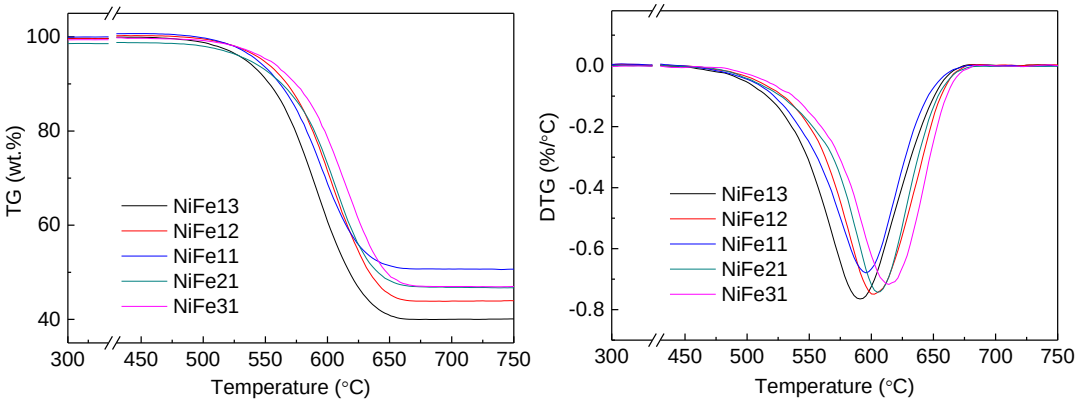

Fig. 5. Temperature program oxidation (TPO) of reacted catalysts.

The carbon residues obtained exhibited very fluffy solid particles (Fig. 6(a)), accumulating a layer with thickness in the range of 10 to 15 mm (the catalyst layer before reaction was 4mm). Fig. 6 also shows the SEM morphology of the synthetized nanomaterials produced with five different catalysts. The filamentous type of carbon could be clearly observed, and only a little proportion of disordered or amorphous carbon were found, which was also suggested by TPO results.

The TEM images shown in Fig. 7 further confirmed that the carbon nanomaterials winded on the surface of catalysts were carbon nanotubes with a tubular-like form. These tubes have outer diameters ranging from 10 to 40 nm with wall thicknesses from 3 to 10 nm. And the length can be up to a few micrometres (at lower magnifications). Encapsulated catalyst nanoparticles can be seen in the middle or at the top of the tubes, while the tube wall extended and coated on the surface of the catalyst particle, forming a closed shell. Two different growth mode of carbon nanotubes have been mentioned according to the metal position [41]. It appears the tip

growth mechanism of CNTs formation was deduced during the catalysis-pyrolysis of plastic wastes in this work. Besides, it can be seen that the diameters of carbon nanotubes are approximately equal to the size of catalyst particles encapsulated in it. It is indicated that the morphology of CNTs is related to the particle size of the catalyst used [42]. And a strong metal-support interaction always lead to well dispersed small catalyst particles [43]. From both SEM and TEM images, the CNTs formed on NiFe21 and NiFe31 were found much thinner than those on NiFe13 and NiFe12, simultaneously the stronger interaction between metal oxides and support was observed at higher Ni to Fe ratio based TPR results. Similar results were also found that, a narrower diameter of filamentous carbon was inclined to be observed with a stronger metal-support interaction of catalyst [44]. In addition, more homogeneous and longer nanotubes were seen in the NiFe31 catalyzed specimen, as shown in Fig. 7(e).

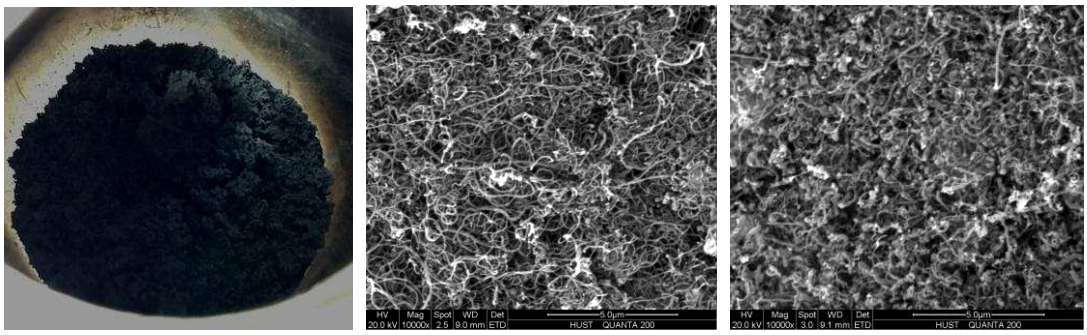

(a) (b) (c)

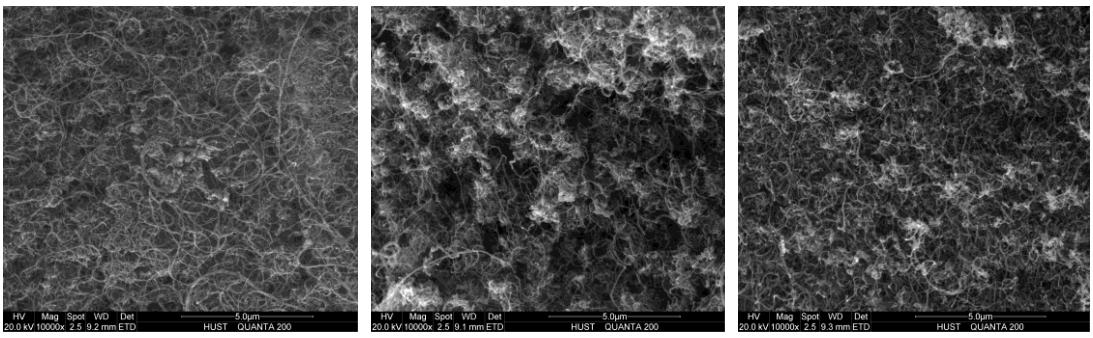

(d) (e) (f)

Fig. 6. Carbon residues after reaction (observation with naked eye) (a) and SEM analysis of reacted catalysts with different Ni to Fe mole ratio (b) NiFe13, (c) NiFe12, (d) NiFe11, (e) NiFe21, (f) NiFe31.

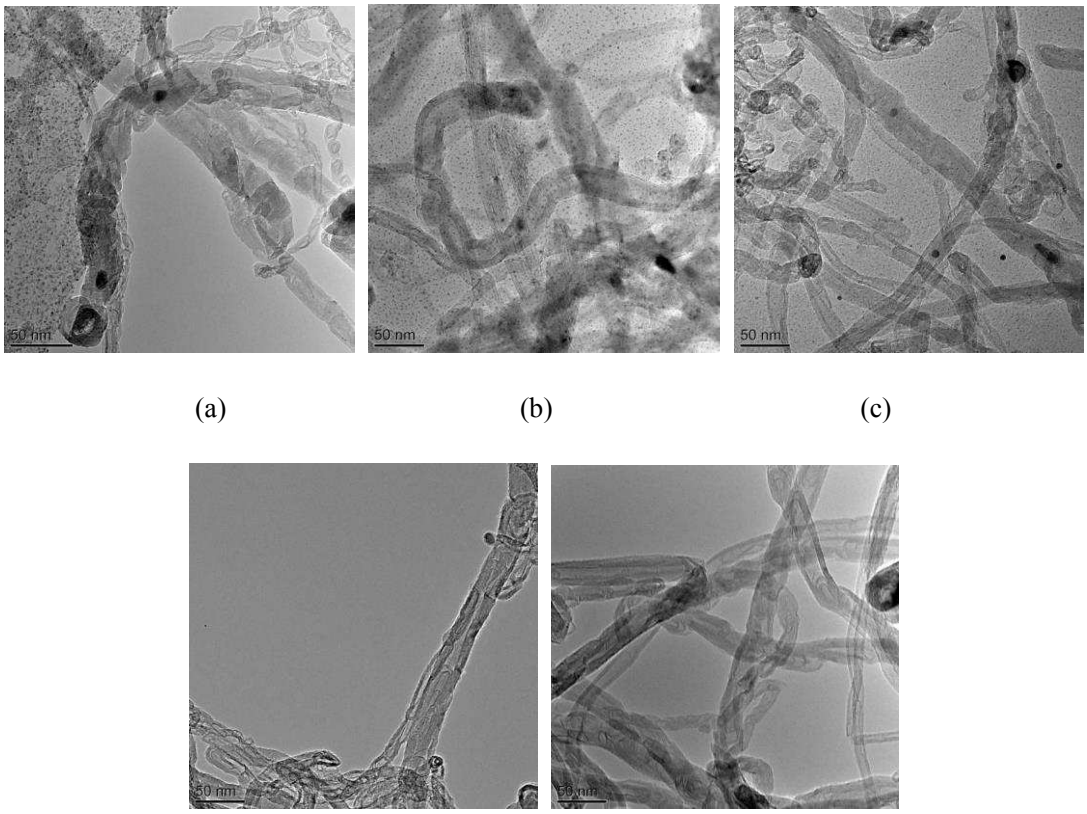

(a) (b) (c)

(d) (e)

Fig. 7. TEM analysis of reacted catalysts with different Ni to Fe mole ratio. (a) NiFe13, (b) NiFe12, (c) NiFe11, (d) NiFe21, (e) NiFe31.

Raman analysis (Fig. 8) was performed to evaluate the structure, crystallinity and graphitization degree of carbons formed over Ni-Fe catalysts during the pyrolysis-catalytic process. The D band around wavelength of 1350 cm^{-1} is ascribed to

408 amorphous or disordered carbon, while the G band at around 1580 cm^{-1} is caused by
409 tangential vibration of the ordered graphite carbon atoms [45]. The peak intensity
410 ratio of I_D/I_G and $I_{G'}/I_G$ are used to estimate the defects and graphitization degree of
411 carbon deposits. It can be seen that all of the current catalysts have the I_D/I_G ratio
412 between 0.64 and 1.03, and the $I_{G'}/ I_G$ ratio from 0.52 to 0.63, comparably with the
413 CNTs in commercial application or with other literatures [46]. In addition, I_D/I_G ratio
414 decreased and $I_{G'}/I_G$ increased at higher ratios of the Ni to Fe catalysts. It appears
415 NiFe21 and NiFe31 have fewer defects than other three catalysts, similar to results
416 observed by TEM. As thermal stability also increased with the increasing ratio of Ni
417 to Fe (from TPO analysis), indicating the thermal stability of carbon is related to the
418 carbon defects (from Raman analysis). Tian et al. [47] also ascribed the good
419 performance of CNTs in heat treatment to the clean and smooth wall surfaces. As for
420 the Ni-Fe catalyst investigated in this work, it can be seen that Ni improves the purity
421 and graphitization degree of carbon nonmaterial.

422 In order to make a comparison between our results and those of literatures, yields
423 of hydrogen and carbon nanotubes using different waste plastics and Ni-Fe based
424 catalysts are gathered in Table 2. Details of morphology and quality of CNTs are also
425 present. It can be seen, compared with other catalysts with similar operation
426 conditions (catalysis temperature: 750 to 800, no steam feeding, fixed bed reactor),
427 bimetallic Ni-Fe catalysts exhibited better performance for simultaneous H_2 and CNTs
428 production from waste polymers. It may because C-C bond cleavage and cracking
429 activity of catalyst were enhanced by using bimetallic catalysts and therefore

increasing H_2 and carbon yields [27]. The relatively lower I_D/I_G also implies better morphology and purity of carbons obtained over Ni-Fe catalyst.

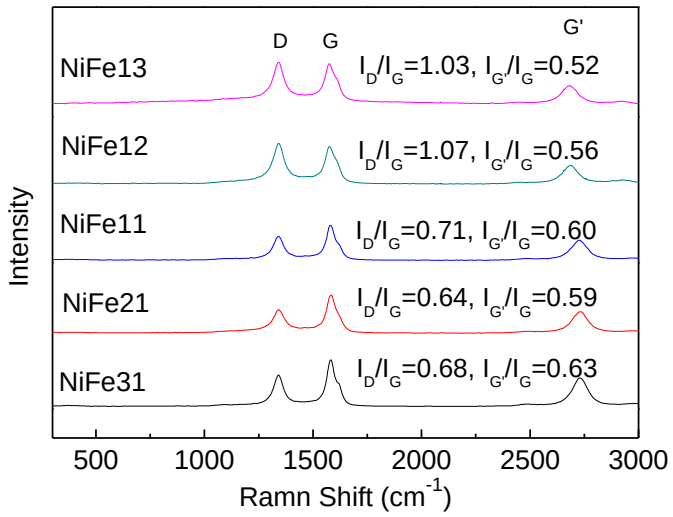

Fig. 8. Raman analysis of the five reacted Ni-Fe catalysts.

Table 2

Comparison of H_2, CNTs yield and Raman indicators between our results and those reported in literatures.

Material	Catalyst	H_2 yield (g/100g sample)	H_2 content (Vol. %)	Carbon (g/100g sample)	I_D/I_G	Source
Mixed plastics	NiFe31/Al_2O_3	7.24	69.98	46	0.68	this work
LDPE	Ni/ Al_2O_3	3.30	58.30	52	0.59	[48]
PS	Ni/ Al_2O_3	2.70	77.20	25	0.93	[48]
PP and PE mixture	H-Ni/ Al_2O_3	5.72	36.13	31	—	[22]
LDPE	Fe/ Al_2O_3	3.90	51.00	27	0.51	[39]
Waste tires	Fe/ Al_2O_3	1.50	33.12	38	0.89	[21]
Mixed plastics	Ni-Mn-Al	12.2	75.6	46	0.9	[10]

4. Conclusions

H_2-rich syngas and high yield of carbon nanotubes were produced with bimetallic Ni-Fe catalysts from real-word waste plastics. The effect of different Ni to Fe molar

ratios during catalyst preparation on the gas product and properties of carbon deposits was studied. The maximum H_2 yield of 8.47 g g^{-1} plastic and H_2 content of 73.93 vol.% were obtained with the NiFe13 catalyst having the highest fraction of Fe. TGA, TEM and Raman analysis have revealed that highly graphitized carbon nanotubes were obtained over all Ni-Fe catalysts. The yield of deposited carbon was related to the metal-support interaction, and higher yield of carbon was obtained for the catalysts with higher Fe loading. However carbon nanotubes with narrower diameters and uniform distributions were grown with higher Ni ratio. The presence of Ni enhanced the thermal stability of the produced carbon products with less carbon defects and higher graphitization degree of carbon, and a higher thermal stability of filamentous carbon over the NiFe31 catalyst was obtained. There is potential flexibility of the bimetallic catalyst for this process, where by adjusting the molar ratio of Ni to Fe the final products can be turned for the production of hydrogen or carbon nanotubes with higher purity.

Acknowledgements

The authors would like to thank the financial support from the National Natural Science Foundation of China (51622604 and 51376076) and the China Postdoctoral Science Foundation (2016M602293). The experiment was also assisted by Analytical and Testing Center in Huazhong University of Science & Technology (http://atc.hust.edu.cn), Wuhan 430074 China.

References

[1] Gu B, Jiang S, Wang H, Wang Z, Jia R, Yang J, et al. Characterization, quantification and management of China's municipal solid waste in spatiotemporal distributions: A review. Waste Management 2016;**61**:67-77.

[2] PlasticsEurope. Plastics - the Facts 2016. 2016.

[3] Sharuddin S D A, Abnisa F, Daud W M A W,Aroua M K. A review on pyrolysis of plastic wastes. Energy Conversion and Management 2016;**115**:308-326.

[4] Miandad R, Barakat M, Aburiazaiza A S, Rehan M,Nizami A. Catalytic pyrolysis of plastic waste: a review. Process Safety and Environmental Protection 2016;**102**:822-838.

[5] Lopez G, Artetxe M, Amutio M, Bilbao J,Olazar M. Thermochemical routes for the valorization of waste polyolefinic plastics to produce fuels and chemicals. A review. Renewable and Sustainable Energy Reviews 2017;**73**:346-368.

[6] Williams P T,Williams E A. Fluidised bed pyrolysis of low density polyethylene to produce petrochemical feedstock. Journal of Analytical and Applied Pyrolysis 1999;**51**:107-126.

[7] Ratnasari D K, Nahil M A,Williams P T. Catalytic pyrolysis of waste plastics using staged catalysis for production of gasoline range hydrocarbon oils. Journal of Analytical and Applied Pyrolysis 2017;**124**:631-637.

[8] Dou B, Wang K, Jiang B, Song Y, Zhang C, Chen H, et al. Fluidized-bed gasification combined continuous sorption-enhanced steam reforming system to continuous hydrogen production from waste plastic. International Journal of Hydrogen Energy 2016;**41**:3803-3810.

[9] Arregi A, Amutio M, Lopez G, Artetxe M, Alvarez J, Bilbao J, et al. Hydrogen-rich gas production by continuous pyrolysis and in-line catalytic reforming of pine wood waste and HDPE mixtures. Energy Conversion and Management 2017;**136**:192-201.

[10] Wu C, Nahil M A, Miskolczi N, Huang J,Williams P T. Processing Real-World Waste Plastics by Pyrolysis-Reforming for Hydrogen and High-Value Carbon Nanotubes. Environmental science & technology 2013;**48**:819-826.

[11] Zhang Y,Williams P T. Carbon nanotubes and hydrogen production from the pyrolysis catalysis or catalytic-steam reforming of waste tyres. Journal of Analytical and Applied Pyrolysis 2016;**122**:490-501.

[12] Wu C, Nahil M A, Miskolczi N, Huang J,Williams P T. Production and application of carbon nanotubes, as a co-product of hydrogen from the pyrolysis-catalytic reforming of waste plastic. Process Safety and Environmental Protection 2016;**103, Part A**:107-114.

[13] Borsodi N, Szentes A, Miskolczi N, Wu C,Liu X. Carbon nanotubes synthetized from gaseous products of waste polymer pyrolysis and their application. Journal of Analytical and Applied Pyrolysis 2016;**120**:304-313.

[14] Iijima S. Helical microtubules of graphitic carbon. Nature 1991.

[15] Baughman R H, Zakhidov A A,de Heer W A. Carbon nanotubes--the route toward applications. Science 2002;**297**:787-792.

[16] De Volder M F, Tawfick S H, Baughman R H,Hart A J. Carbon nanotubes: present and future commercial applications. Science 2013;**339**:535-539.

[17] Shah K A,Tali B A. Synthesis of carbon nanotubes by catalytic chemical vapour deposition: A review on carbon sources, catalysts and substrates. Materials Science in Semiconductor Processing 2016;**41**:67-82.

[18] Uddin M N, Daud W W,Abbas H F. Co-production of hydrogen and carbon nanofibers from

methane decomposition over zeolite Y supported Ni catalysts. Energy Conversion and Management 2015;**90**:218-229.

[19] Wu C F, Wang Z C, Huang J,Williams P T. Pyrolysis/gasification of cellulose, hemicellulose and lignin for hydrogen production in the presence of various nickel-based catalysts. Fuel 2013;**106**:697-706.

[20] Yao D, Hu Q, Wang D, Yang H, Wu C, Wang X, et al. Hydrogen production from biomass gasification using biochar as a catalyst/support. Bioresource Technology 2016;**216**:159-164.

[21] Zhang Y, Wu C, Nahil A,Williams P T. Pyrolysis-Catalytic Steam Reforming/Gasification of Waste Tires for Production of Carbon Nanotubes and Hydrogen. Energy & Fuels 2015.

[22] Yang R-X, Chuang K-H,Wey M-Y. Effects of nickel species on Ni/Al2O3 catalysts in CNTs and hydrogen production by waste plastics gasification: Bench-scale and pilot-scale tests. Energy & Fuels 2015.

[23] Pudukudy M, Yaakob Z,Takriff M S. Methane decomposition into COx free hydrogen and multiwalled carbon nanotubes over ceria, zirconia and lanthana supported nickel catalysts prepared via a facile solid state citrate fusion method. Energy Conversion and Management 2016;**126**:302-315.

[24] Acomb J C, Wu C,Williams P T. The use of different metal catalysts for the simultaneous production of carbon nanotubes and hydrogen from pyrolysis of plastic feedstocks. Applied Catalysis B: Environmental 2016;**180**:497-510.

[25] Popovska N, Danova K, Jipa I,Zenneck U. Catalytic growth of carbon nanotubes on zeolite supported iron, ruthenium and iron/ruthenium nanoparticles by chemical vapor deposition in a fluidized bed reactor. Powder Technology 2011;**207**:17-25.

[26] Cartwright R, Esconjauregui S, Hardeman D, Bhardwaj S, Weatherup R, Guo Y, et al. Low temperature growth of carbon nanotubes on tetrahedral amorphous carbon using Fe–Cu catalyst. Carbon 2015;**81**:639-649.

[27] Kaya B, Irmak S, Hasanoğlu A,Erbatur O. Developing Pt based bimetallic and trimetallic carbon supported catalysts for aqueous-phase reforming of biomass-derived compounds. International Journal of Hydrogen Energy 2015;**40**:3849-3858.

[28] Shen Y, Zhao P, Shao Q, Takahashi F,Yoshikawa K. In situ catalytic conversion of tar using rice husk char/ash supported nickel–iron catalysts for biomass pyrolytic gasification combined with the mixing-simulation in fluidized-bed gasifier. Applied Energy 2015;**160**:808-819.

[29] Wei G, He F, Zhao Z, Huang Z, Zheng A, Zhao K, et al. Performance of Fe–Ni bimetallic oxygen carriers for chemical looping gasification of biomass in a 10 kWth interconnected circulating fluidized bed reactor. International Journal of Hydrogen Energy 2015;**40**:16021-16032.

[30] Shen W, Huggins F E, Shah N, Jacobs G, Wang Y, Shi X, et al. Novel Fe–Ni nanoparticle catalyst for the production of CO- and CO2-free H2 and carbon nanotubes by dehydrogenation of methane. Applied Catalysis A: General 2008;**351**:102-110.

[31] Yao D, Wu C, Yang H, Hu Q, Nahil M A, Chen H, et al. Hydrogen production from catalytic reforming of the aqueous fraction of pyrolysis bio-oil with modified Ni–Al catalysts. International Journal of Hydrogen Energy 2014;**39**:14642-14652.

[32] Al-Dossary M,Fierro J. Effect of high-temperature pre-reduction in Fischer–Tropsch synthesis on Fe/ZrO 2 catalysts. Applied Catalysis A: General 2015;**499**:109-117.

[33] Sepúlveda R, Plunk A A,Dunand D C. Microstructure of Fe 2 O 3 scaffolds created by freeze-casting and sintering. Materials Letters 2015;**142**:56-59.

[34] de Freitas Silva T, Dias J A C, Maciel C G,Assaf J M. Ni/Al 2 O 3 catalysts: effects of the promoters Ce, La and Zr on the methane steam and oxidative reforming reactions. Catalysis Science & Technology 2013;**3**:635-643.

[35] Alipour Z, Rezaei M,Meshkani F. Effects of support modifiers on the catalytic performance of Ni/Al 2 O 3 catalyst in CO 2 reforming of methane. Fuel 2014;**129**:197-203.

[36] Valle B, Aramburu B, Remiro A, Bilbao J,Gayubo A G. Effect of calcination/reduction conditions of Ni/La 2 O 3–αAl 2 O 3 catalyst on its activity and stability for hydrogen production by steam reforming of raw bio-oil/ethanol. Applied Catalysis B: Environmental 2014;**147**:402-410.

[37] Gallego G S, Barrault J, Batiot-Dupeyrat C,Mondragón F. Production of hydrogen and MWCNTs by methane decomposition over catalysts originated from LaNiO 3 perovskite. Catalysis Today 2010;**149**:365-371.

[38] Nahil M A, Wu C,Williams P T. Influence of metal addition to Ni-based catalysts for the co-production of carbon nanotubes and hydrogen from the thermal processing of waste polypropylene. Fuel Processing Technology 2015;**130**:46-53.

[39] Acomb J C, Wu C,Williams P T. Effect of growth temperature and feedstock: catalyst ratio on the production of carbon nanotubes and hydrogen from the pyrolysis of waste plastics. Journal of Analytical and Applied Pyrolysis 2015.

[40] Sivakumar V, Abdullah A Z, Mohamed A R,Chai S-P. Optimized parameters for carbon nanotubes synthesis over Fe and Ni catalysts VIA methane CVD. Rev. Adv. Mater. Sci 2011;**27**:25-30.

[41] Huang S, Woodson M, Smalley R,Liu J. Growth mechanism of oriented long single walled carbon nanotubes using “fast-heating” chemical vapor deposition process. Nano Letters 2004;**4**:1025-1028.

[42] Chung Y-H,Jou S. Carbon nanotubes from catalytic pyrolysis of polypropylene. Materials chemistry and physics 2005;**92**:256-259.

[43] Cargnello M, Doan-Nguyen V V, Gordon T R, Diaz R E, Stach E A, Gorte R J, et al. Control of metal nanocrystal size reveals metal-support interface role for ceria catalysts. Science 2013;**341**:771-773.

[44] Yeoh W-M, Lee K-Y, Chai S-P, Lee K-T,Mohamed A R. Effective synthesis of carbon nanotubes via catalytic decomposition of methane: Influence of calcination temperature on metal–support interaction of Co–Mo/MgO catalyst. Journal of Physics and Chemistry of Solids 2013;**74**:1553-1559.

[45] Gong J, Liu J, Wan D, Chen X, Wen X, Mijowska E, et al. Catalytic carbonization of polypropylene by the combined catalysis of activated carbon with Ni 2 O 3 into carbon nanotubes and its mechanism. Applied Catalysis A: General 2012;**449**:112-120.

[46] Awadallah A E, Aboul-Enein A A,Aboul-Gheit A K. Effect of progressive Co loading on commercial Co–Mo/Al 2 O 3 catalyst for natural gas decomposition to COx-free hydrogen production and carbon nanotubes. Energy Conversion and Management 2014;**77**:143-151.

[47] Tian F, Li H, Zhao N,He C. Catalyst effects of fabrication of carbon nanotubes synthesized by chemical vapor deposition. Materials chemistry and physics 2009;**115**:493-495.

[48] Acomb J C, Wu C,Williams P T. Control of steam input to the pyrolysis-gasification of waste plastics for improved production of hydrogen or carbon nanotubes. Applied Catalysis B: Environmental 2014;**147**:571-584.